N,*N*'-linked urea oligomers : synthesis, conformational studies and self-assembly properties.

The functional diversity in proteins, although mediated by sophisticated tertiary and quaternary structures, relies on a small set of distinct secondary structural elements: sheets, helices and turns. Search for new nonnatural oligomers ("foldamers")[1] designed to reproduce or mimic the essential protein features have gained considerable interest with potential application in pharmaceutical research. Seminal works published by the groups of *Seebach, Gellman* and *Hanessian* have revealed that short peptides made exclusively with enantiopure β- or γ-amino acids, correctly substituted, could form stable helical or pleated-sheet-type structures in solution and in the solid state[1] (Figure 1).

My memory of thesis is devoted to the synthesis and the conformational study of linear and cyclic *N*,*N*'-linked urea oligomers. The linear *N*,*N*'-linked urea oligomers of general formula **B** have a strong analogy with γ-peptides such as **A**. However, their conformational preference as their folding propensity were not yet studied.

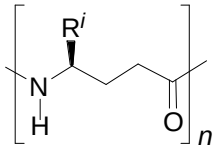

A

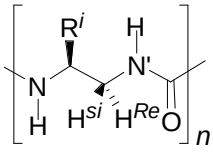

B

A simple and effective method was developed to obtain succinimidyl carbamates derivatives **4** starting from β-amino acids **1** (Scheme 1). Briefly, the *N*-protected β[3] amino acid, were first converted to the corresponding acyl azides, and following Curtius rearrangement, the resulting isocyanates were treated with *N*-hydroxysuccinimide to give The Boc or Fmoc protected carbamates **4a-m** in good yields (51-86%, Table 1). These precursors were used for the synthesis of linear *N*,*N*'-linked urea oligomers by solid phase methodology[2] (Scheme 2). The oligoureas were assembled on Rink amide resin *via* successive coupling and deprotection cycles. By this way, several oligoureas were synthezised (Scheme 3). The purity of crudes oligomers, obtained after cleavage from the

resin and lyophilisation raised from 35 for **8** to 63% for **6** as checked by reversed-phase HPLC. Oligomers **6**, **7** and **8** were purified by reversed-phase HPLC (C_{18}) to a final purity >95% and lyophilized.

The conformational study in solution of these linear *N,N*'-linked urea oligomers was performed by NMR (DQF-COSY, TOCSY, and ROESY) in pyridin-d_5 and shows that the oligomeric molecule **7** adopt a helicoidal secondary structure. The secondary structure of the heptaurea **7** is a right-handed 2.5 helix with a pitch of approximatively 5.1 Å (Figure 2) that is well defined for residues 2–6. Although the structure shares overall similarity with the helical backbone of γ-peptides, the helix of **7** displays a more complicated intramolecular hygrogen-bonding pattern that is characterized by the simultenaous presence of 12- and 14-membered pseudocycles resulting from $C{=}O_i\cdots HN'_{i+2}$ and $C{=}O_i\cdots HN_{i+3}$ hydrogen bonds (Figure 3). Essentially two factors may play a role in inducing and stabilizing the 2.5 helix: *i*) a rigid (+)-*syn*-clinal arrangement around the C(*a*)-C(*b*) bound very similar to what was previously observed for β-peptides and γ-peptides, and *ii*) intramolecular H-bonds : $C{=}O_i\cdots HN'_{i+2}$ and $C{=}O_i\cdots HN_{i+3}$. NMR studies in pyridin-d_5 revealed that the nonamer oligourea **8** adopts the regular (*P*)-2.5 helical secondary structure (Figure 4) very similar to that determined for the oligourea heptamer **7** (see Figure 5) and closely related to the (*P*)-2.6_{14} helix of γ-peptides. Thus, the similarity between γ-peptides and *N,N*'-linked oligoureas is no longer restricted to an isosteric relationship (based exclusively on the chemical formulae of the backbone) but is extended to a unique three dimensional structural relationship. In addition CD spectra of **8** (0.2 mM in MeOH) were recorded with the aim to gain more information about oligoureas. In contrast to 2,6-helical γ-peptides, which display only a weak or no Cotton effect, oligoureas exhibit an intense positive Cotton effect at *ca.* 203 nm that decreases only slowly upon increasing the temperature.

Additionally, helical oligoureas may serve as scaffolds for *de novo* design of molecules with interesting biological activities. We screened for antimicrobial activity by incubating of various concentrations (1.5 to 800 $\mu g.mL^{-1}$ of oligoureas **6**, **7** and **8**) with different eukaryotic and prokaryotic microorganisms[5]. The standard measurement of antibacterial potency of a compound is the minimum concentration (MIC), required for complete inhibition of growth. The result of this study are presented in Table 2. One of these

oligoureas (nonamer **8**) exhibits a strong antimicrobial activities (Gram-negative : *Escherichia Coli*, *Salmonella cloacae*, *Pseudomonas aeruginosa* and Gram positive : *Staphylococcus aureus*, *Micrococcus luteus*) with a poor hemolytic effect.

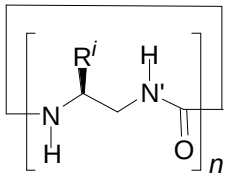

C

Assembly of self-complementary cyclo-oligomeric subunits through noncovalent processes (i.e. hydrogen bonding, aromatic stacking) has emerged as a powerful strategy to generate artificial organic nanotubular structures. We envisioned that the corresponding macrocyclic of general formula **C** derivatives might lead to flat ring structures with a high degree of self-complementarity that would allow self-assembling processes to occur. The succinimidyl carbamate derivatives were used for the synthesis of cyclic *N*,*N*'-linked urea oligomers in solution. The general strategy used to synthesize the 20-membered-ring macrocycle **17** is outlined in scheme 4. Single crystals of **17** suitable for X-ray studies were grown by slow evaporation of the EtOH solution. The assembly properties of these compounds were analysed in the solid state. X-ray cristallographic analysis revealed that cyclourea **17** adopts a C_4-symetric conformation and stacks to form a hollow tubular structure[6]. The four urea fragments in the macrocycle present an all-trans, planar conformation with all the urea carbonyl groups pointing down and all the NH groups pointing up (Figure 7). The macrocycle exhibits a square shape with a cross-section of 6.052(7) Å distance between C1A and C1B). Particularly noteworthy is the presence of the density inside the tubular cavity wich modeled as disordered water molecules at overlapping sites.

In conclusion, by determining the solution structure of the heptamer **7** and the nonamer **8**, we have demonstrated that *N*,*N*'-linked oligoureas of general formula **B** belong to the growing family of non-natural peptide oligomers (i.e. foldamers) with defined and predictable secondary structures. The knowledge of the three-dimentional stucture of oligoureas will be useful for the de novo design of oligomers with controlled shape and

defined biological activities (i.e. antimicrobial oligoureas). Moreover, we have shown that cyclic units of oligourea self-assemble in the crystal state to form hydrogen-bounded polar nanotubes.

[1] For review on foldamers see D. J. Hill, M. J. Mio, R. B. Prince, T. S. Hughes, J. S. Moore, *Chem. Rev.* **2001**, *101*, 3893-4011. and references herein.

[2] G. Guichard, V. Semetey, C. Didierjean, A. Aubry, J. P. Briand, M. Rodriguez, *J. Org. Chem.* **1999**, 64, 8702-8705.

[3] G. Guichard, V. Semetey, M. Rodriguez, J. P. Briand, *Tetrahedron Lett*. **2000**, 41, 1553-1557.

[4] V. Semetey, D. Rognan, C. Hemmerlin, R. Graff, J. P. Briand, M. Marraud, G. Guichard, *Angew. Chem. Int. Ed*. **2002**, 41, 1893-1895.

[5] To be published.

[6] C. Hemmerlin, M. Marraud, D. Rognan, R. Graff, V. Semetey, J. P. Briand, G. Guichard, *Helvetica Chimica Acta* 2002, 85, 3692-3711.

[7] V. Semetey, C. Didierjean, J. P. Briand, A. Aubry, G. Guichard, *Angew. Chem. Int. Ed.* **2002**, 41, 1895-1898.

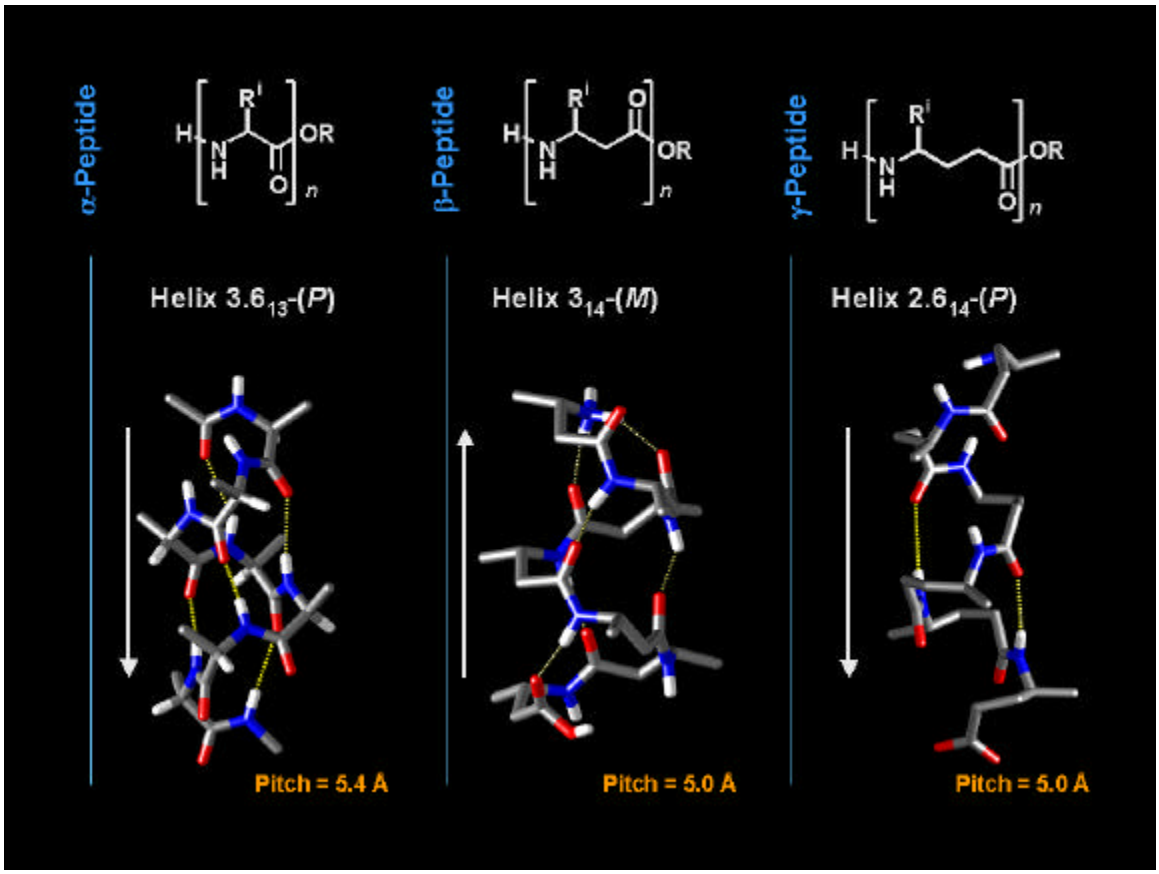

Figure 1. Comparison of the helical secondary structures and H-bonding patterns of *a*-, *b*- and *g*- peptides.

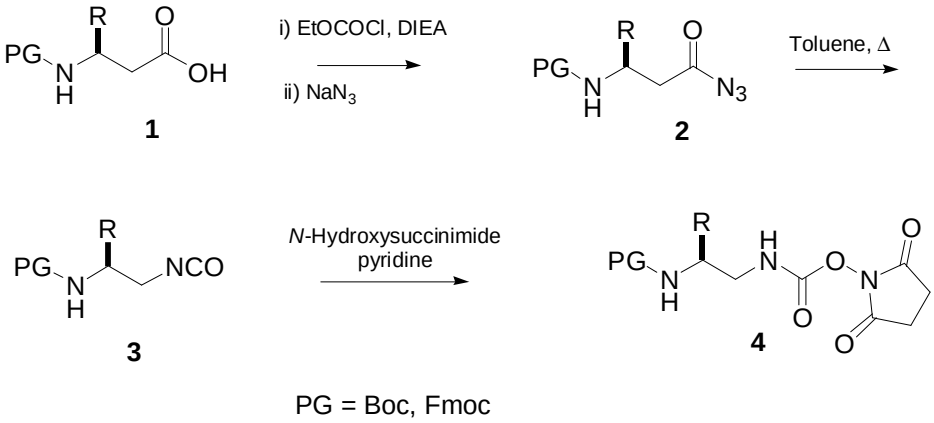

Scheme 1. Synthesis of succinimidyl carbamate derivatives starting from *b*-amino acids. DIEA = diisopropylethylamine.

	PG	R	Yield (%)	m.p.(ºC)	RP-HPLC R_t (min)
4a	Boc	H	55	132-134	6.95[a]
4b		Me	60	153-155	8.00[a]
4c		*I*Pr	51	125-127	10.80[a]
4d		Bn	55	163-164	12.79[a]
4e		CH_2COOBn	58	115-117	13.47[a]
4f		CH(Me)OBn	64	109-110	14.59[a]
4g		$(CH_2)_4NHBoc$	60	116-119	10.63[a]
4h	Fmoc	Me	86	161-163	10.44[b]
4i		*i*Pr	56	109-11	11.84[b]
4j		*i*Bu	51	134-137	12.63[b]
4k		Bn	66	175-177	12.48[b]
4l		Bn(O*t*Bu)	78	138-140	13.87[b]
4m		$(CH_2)_4NHBoc$	79	122-124	12.67[b]

[a] linear gradient of *A* (0.1% TFA in H_20) and *B* (MeCN containing 0.08% TFA), 20-80% *B*, 20 min. [b] 30-100% *B*, 20 min.

Table 1. Conversion of *b*-amino acids **1** to the corresponding succinimidyl carbamates **4a-m**.

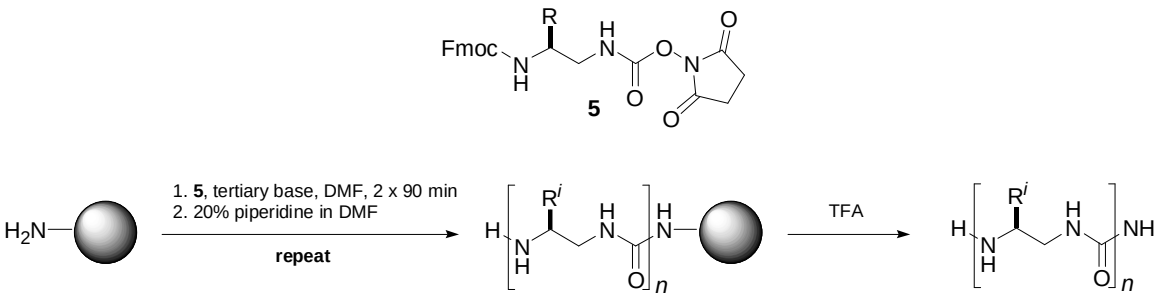

Scheme 2. General procedure for the solid phase synthesis of oligoureas using succinimidyl carbamates **4**. DMF = dimethylformamide, TFA = trifluoroacetic acid.

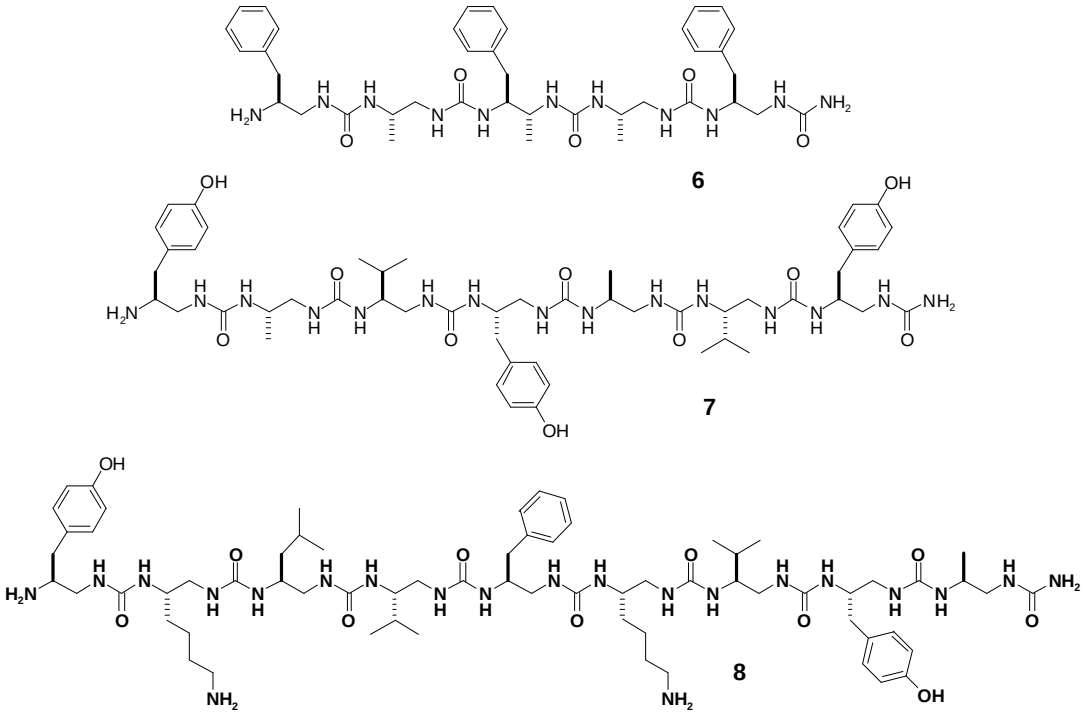

Scheme 3. Oligoureas synthesized on solid support.

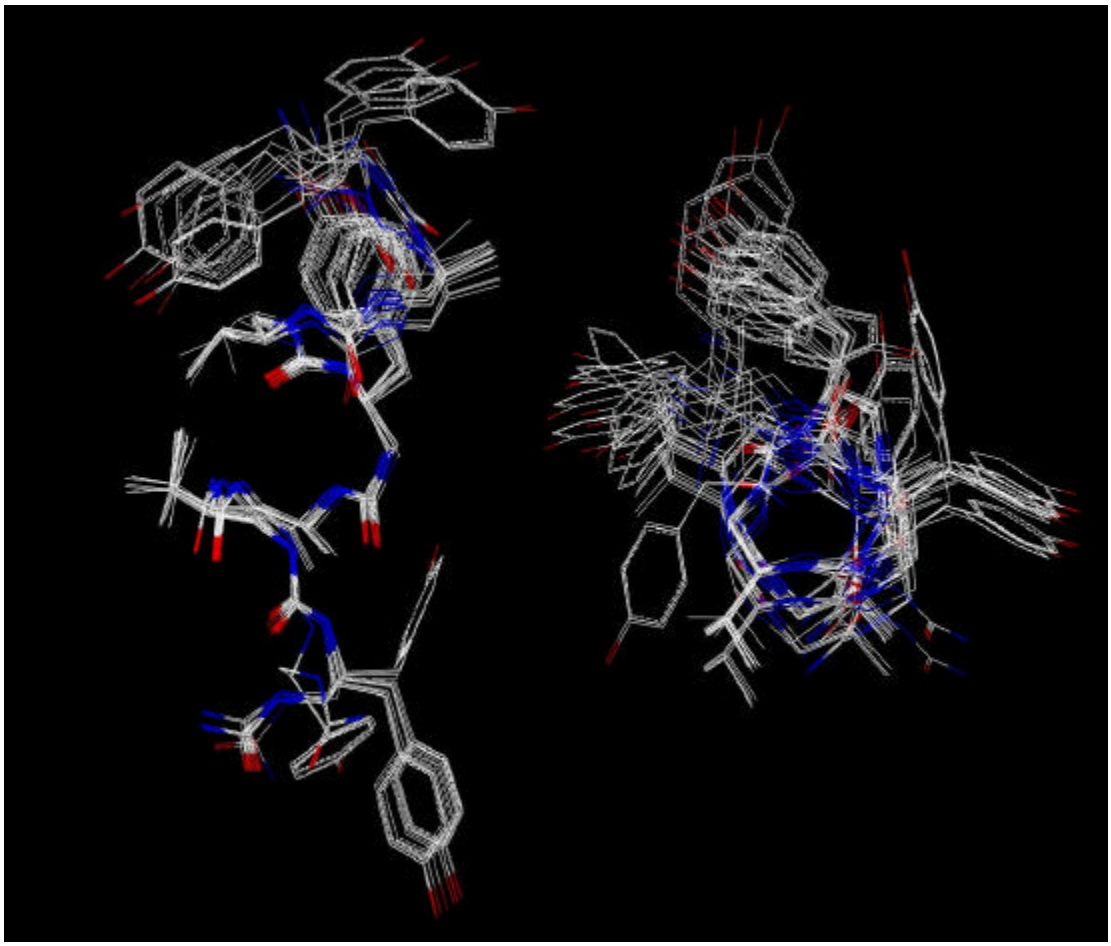

Figure 2. Bundle of the 20 best structures of the lowest energy A) viewed along the helix axis, and B) top view. Root-mean-square (rms) differences of the bond and angle deviations from ideality were less than 0.02 Å and 3º, respectively. Rms deviations for al heavy backbone atoms from a mean structure were 0.56±0.18 for residues 1–7 and 0.36±0.19 Å for residues 2–7.

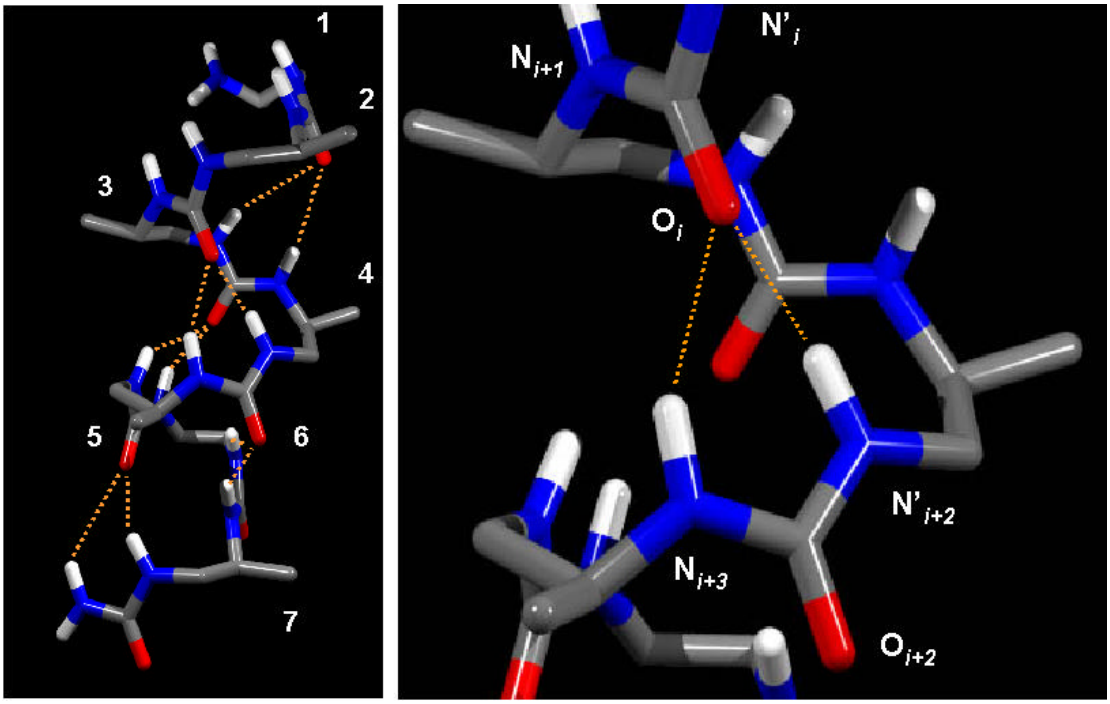

Figure 3. Atom numbering and schematic representation of the hydrogen-bonding pattern as found in the 2.5 helix of heptaoligourea **7**.

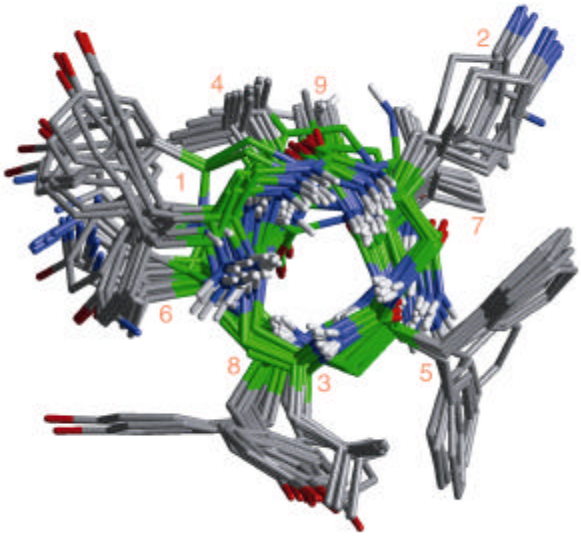

Figure 4. NMR structure of the oligourea **8** in pyridin-d_5 (top view). Bundle of the 20 best structures of lowest energy.

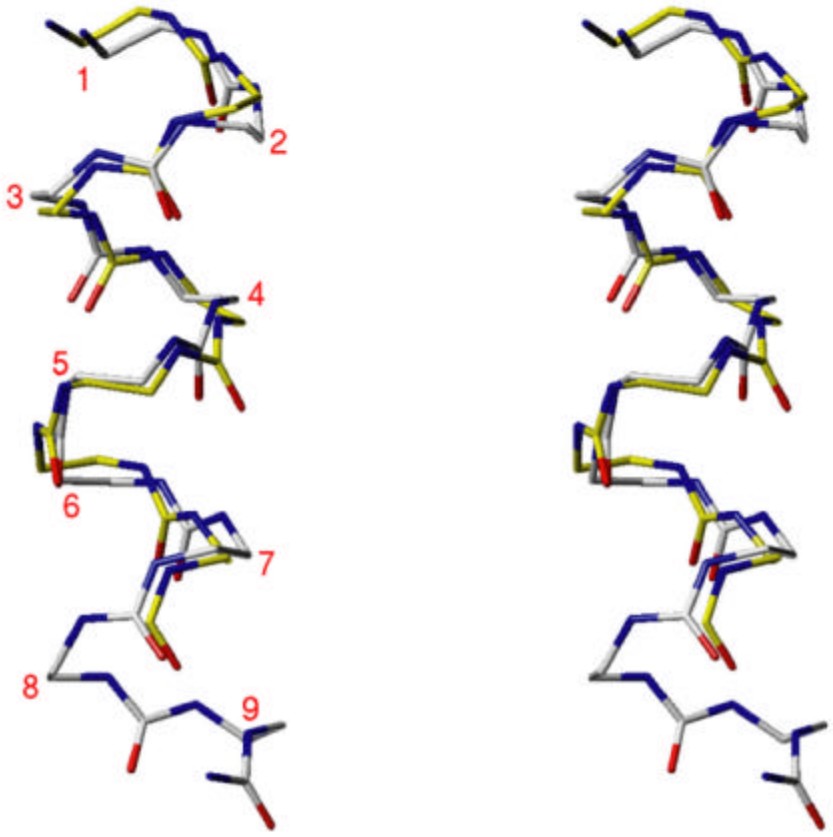

Figure 5. Overlay of the backbone structures of heptamer **7** and of the nonamer **8**, both in pyridin-d_5 (stereo view). C-Atoms of the 7-mer and of the 9-mer are displayed in yellow and white, respectively. Rms deviations of all heavy backbone atoms are 0.60 Å for residues 1-7.

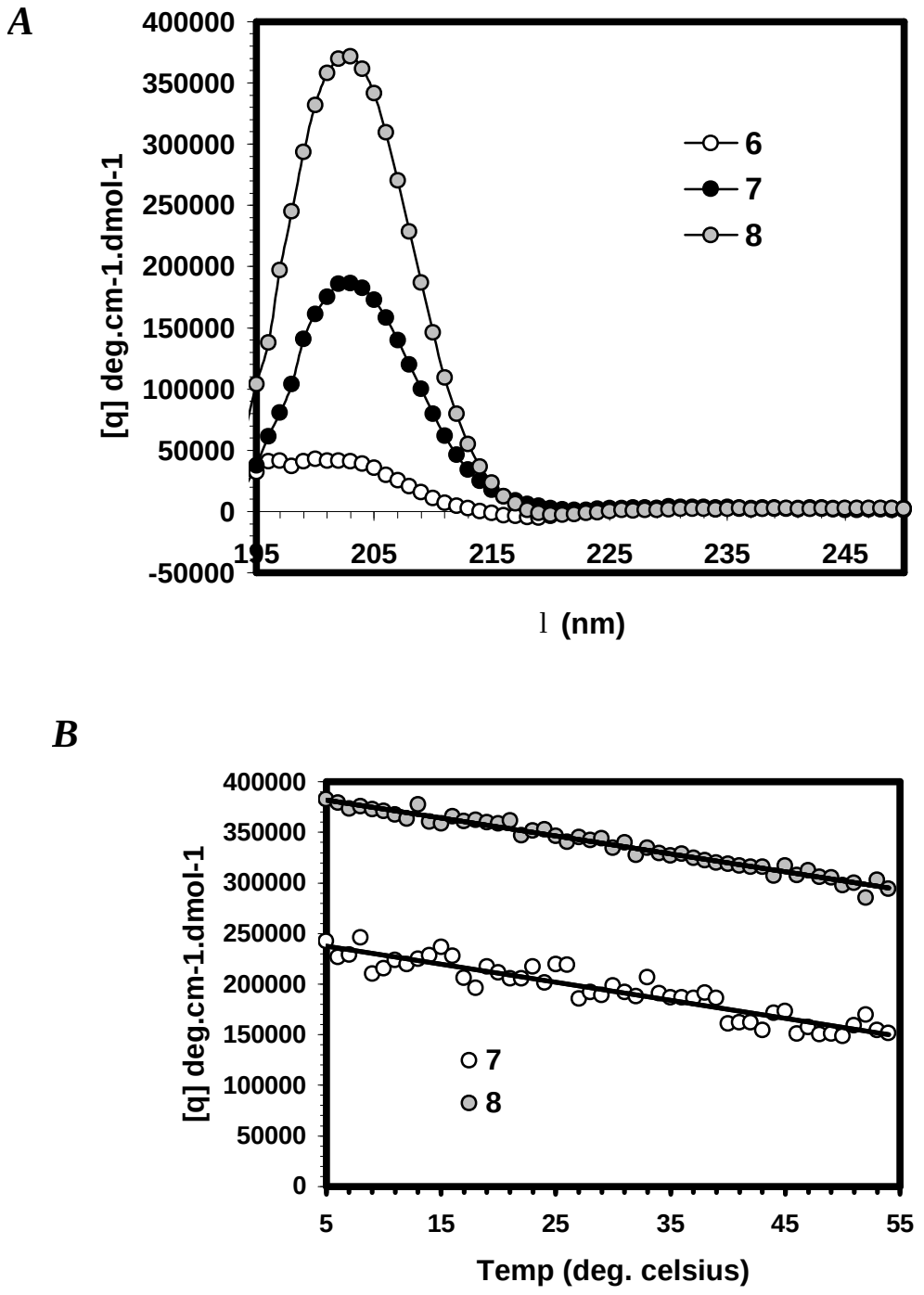

Figure 6. ***A***) CD spectrum of oligoureas 6, 7 and 8 recorded in MeOH at room temperature at a concentration of 0.2 mM. ***B***) CD Temperature scan of 7 and 8 in MeOH for λ = 203 nm. Molar ellipticity q in deg.cm^{-1}.dmol^{-1}.

MIC[a] ($\mu g.mL^{-1}$)	**8**	**7**	**6**
Escherichia Coli	4.1	>100	>100
Staphylococcus aureus	8.1	N.D.	N.D.
Salmonella cloacae	4.1	N.D.	N.D.
Micrococcus luteus	4.1	>100	>100
Pseudomonas aeruginosa	32.5	N.D.	N.D.
Aspergillus fumigatus	>100	N.D.	N.D.
Neurospora crassa	32.5	>100	>100

Table 2. Minimal inhitory concentration (MIC, in $\mu g.mL^{-1}$) for oligoureas **6**, **7** and **8**.

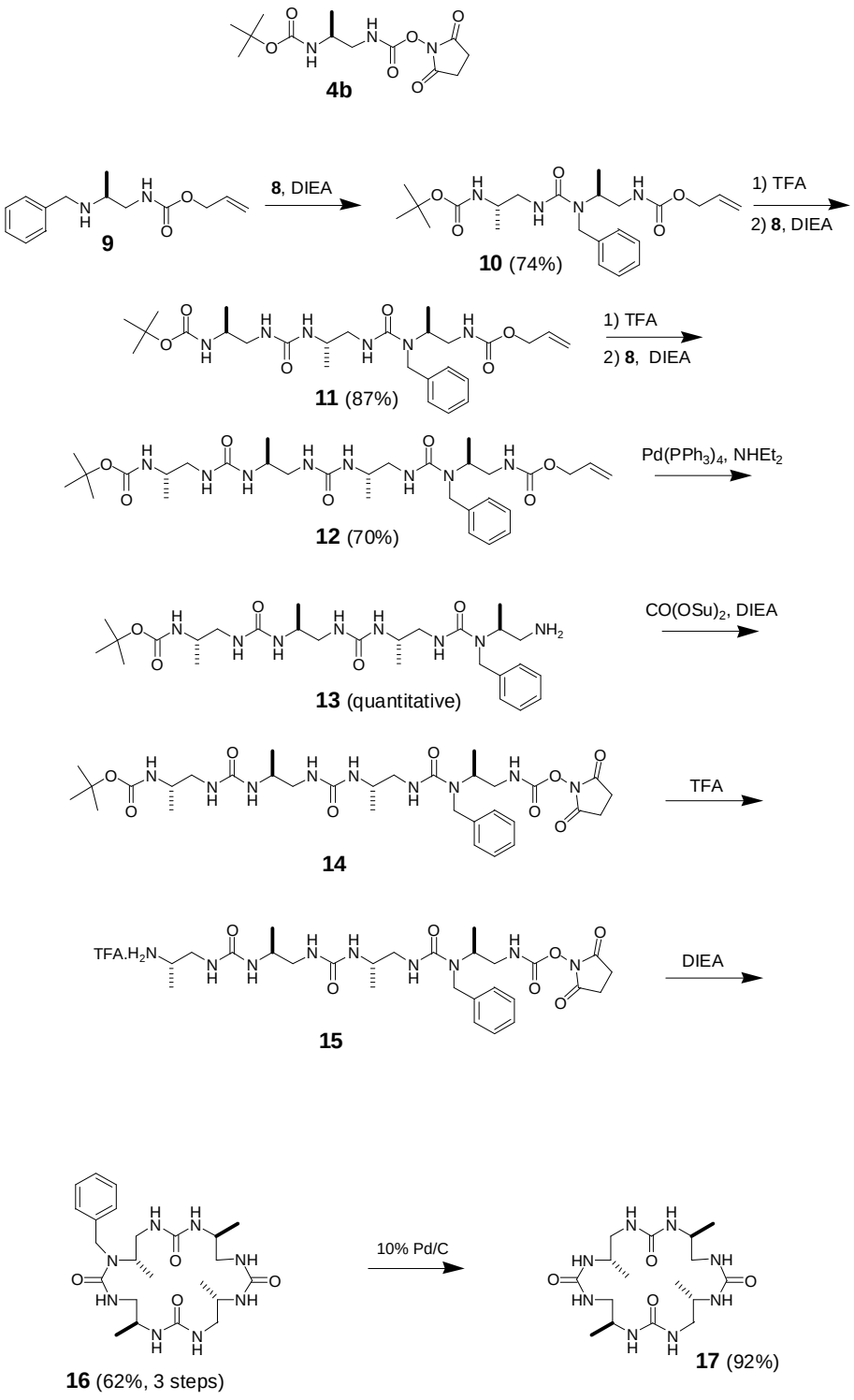

Scheme 4. Synthesis of **17**. DIEA = diisopropylethylamine, Su = succinimidyl, TFA = Trifluoroacetic acid.

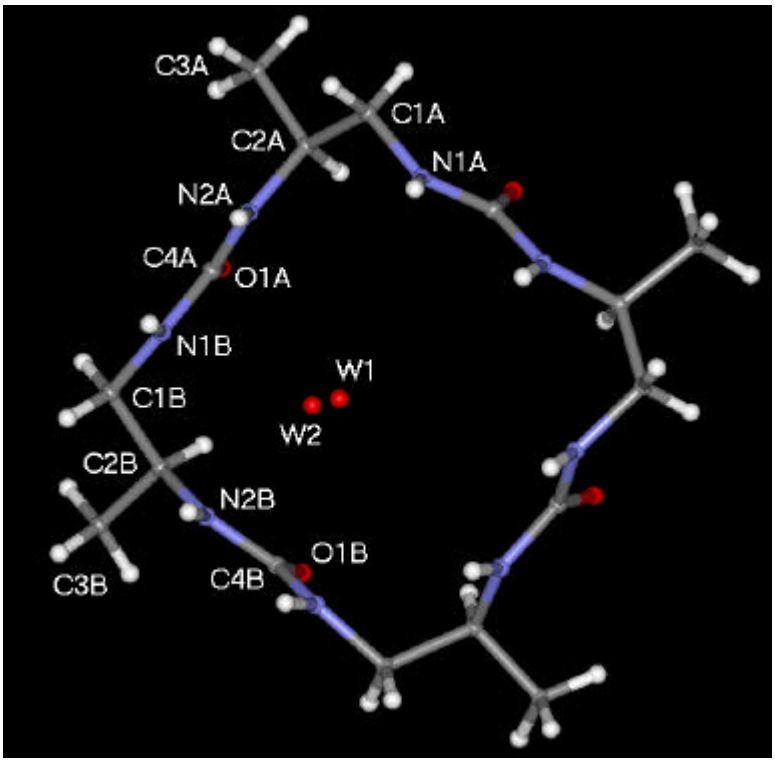

Figure 7. Ball and stick representation of **17** showing the numbering scheme. The torsion angles [º] of the main chain are : N1A-C1A-C2A-N2A 57.9(2), C1A-C2A-N2A-C4A –156.7(2), C2A-N2A-C4A-N1B 177.4(2), N2A-C4A-N1B-C1B 172.6(2), C4A-N1B-C1B-C2B 78.0(3).

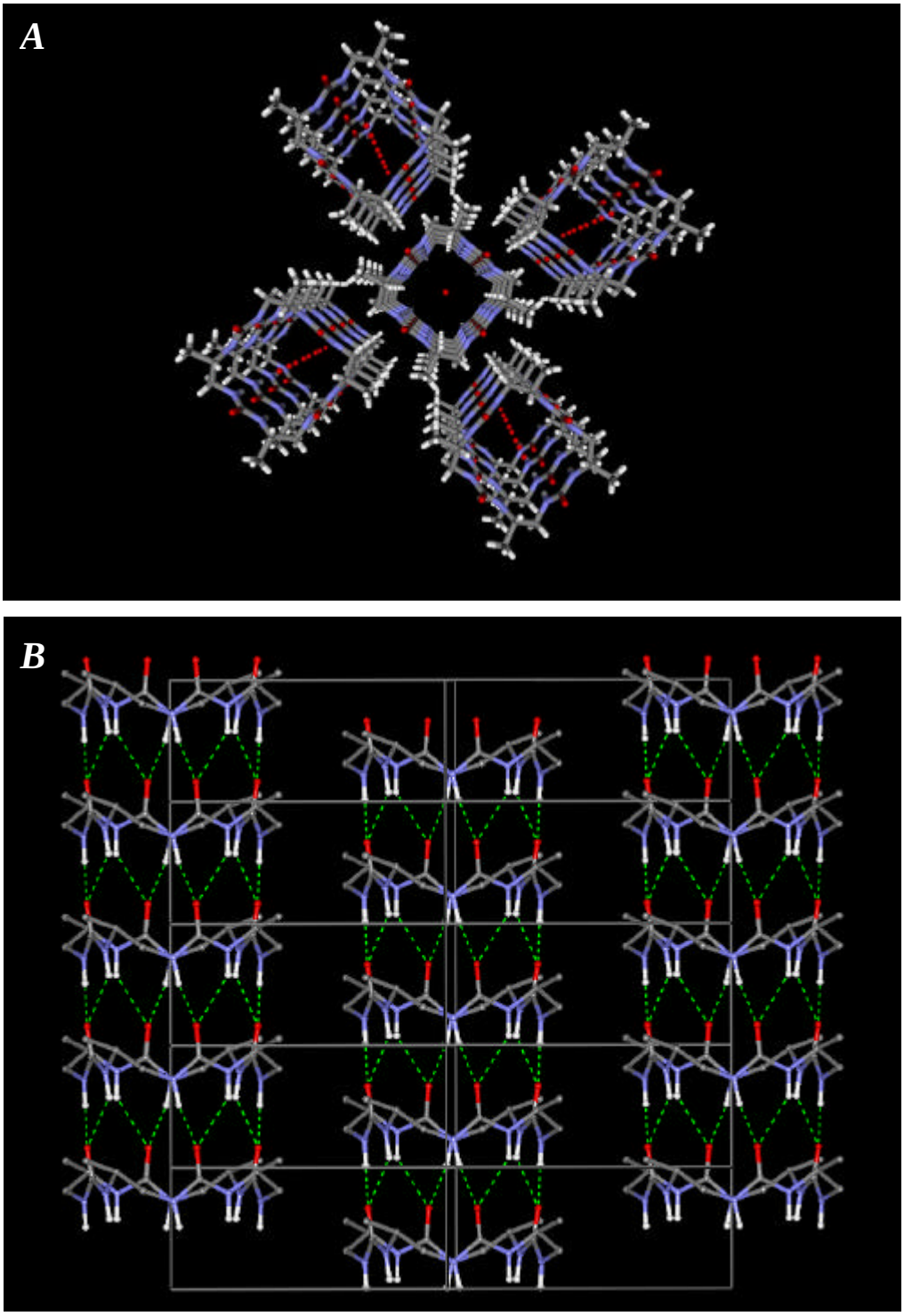

Figure 7. Views of the tubular organization of **17**: ***A***) view along the channel axis. ***B***) Perpendicular view to the channel axis. The intermolecular hydrogen bonds are marked as dashed lines. The solvent molecules and H atoms, except those of the NH groups, are omitted for clarity. The edges of the unit cells are represented in gray.